Selective lesion of retrotrapezoid Phox2b-expressing neurons raises the apnoeic threshold in rats

Ana C. Takakura[1], Thiago S. Moreira[1], Ruth L. Stornetta[2], Gavin H. West[2], Justin M. Gwilt[2] and Patrice G. Guyenet[2]

[1]*Department of Physiology, UNIFESP-EPM, São Paulo, SP, 04023-060, Brazil*
[2]*Department of Pharmacology, University of Virginia, Charlottesville, VA 22908, USA*

Injection of the neurotoxin saporin–substance P (SSP-SAP) into the retrotrapezoid nucleus (RTN) attenuates the central chemoreflex in rats. Here we ask whether these deficits are caused by the destruction of a specific type of interneuron that expresses the transcription factor Phox2b and is non-catecholaminergic (Phox2b$^+$TH$^-$). We show that RTN contains around 2100 Phox2b$^+$TH$^-$ cells. Injections of SSP-SAP into RTN destroyed Phox2b$^+$TH$^-$ neurons but spared facial motoneurons, catecholaminergic and serotonergic neurons and the ventral respiratory column caudal to the facial motor nucleus. Two weeks after SSP-SAP, the apnoeic threshold measured under anaesthesia was unchanged when fewer than 57% of the Phox2b$^+$TH$^-$ neurons were destroyed. However, destruction of $70 \pm 3.5\%$ of these cells was associated with a dramatic rise of the apnoeic threshold (from 5.6 to 7.9% end-expiratory P_{CO_2}). In anaesthetized rats with unilateral lesions of around 70% of the Phox2b$^+$TH$^-$ neurons, acute inhibition of the contralateral intact RTN with muscimol instantly eliminated phrenic nerve discharge (PND) but normal PND could usually be elicited by strong peripheral chemoreceptor stimulation (8/12 rats). Muscimol had no effect in rats with an intact contralateral RTN. In conclusion, the destruction of the Phox2b$^+$TH$^-$ neurons is a plausible cause of the respiratory deficits caused by injection of SSP-SAP into RTN. Two weeks after toxin injection, 70% of these cells must be killed to cause a severe attenuation of the central chemoreflex under anaesthesia. The loss of an even greater percentage of these cells would presumably be required to produce significant breathing deficits in the awake state.

The retrotrapezoid nucleus (RTN) contributes to an unknown extent to the central chemoreflex (the activation of breathing by elevation of CNS P_{CO_2}) (Feldman *et al.* 2003; Nattie & Li, 2008). Neurophysiological and genetic evidence suggests that the RTN neurons involved in this reflex are a group of chemosensitive glutamatergic interneurons that express the transcription factor Phox2b and lack tyrosine-hydroxylase (henceforth called RTN Phox2b$^+$TH$^-$ neurons) (Amiel *et al.* 2003; Weese-Mayer *et al.* 2005; Stornetta *et al.* 2006; Mulkey *et al.* 2007*b*; Dubreuil *et al.* 2008).

Participation in the chemoreflex may be only one aspect of the role of the Phox2b$^+$TH$^-$ neurons in breathing. Acute bilateral inhibition of RTN neurons under anaesthesia eliminates breathing, an effect that is not reversed by

raising CO_2 (Takakura *et al.* 2006). The genetic deletion of the Phox2b$^+$TH$^-$ neurons produces a dramatic reduction of the resting level of breathing in addition to the loss of the chemoreflex (Dubreuil *et al.* 2008). These results suggest that the level of activity of the Phox2b$^+$TH$^-$ neurons of RTN could be defining the intensity of involuntary breathing. This hypothesis is compatible with the known integrative properties of the Phox2b$^+$TH$^-$ neurons *in vivo*. Indeed these acid-sensitive excitatory cells are also powerfully activated by inputs from peripheral chemoreceptors and from the raphe, and their activity is regulated by inputs from the lungs (Takakura *et al.* 2006; Moreira *et al.* 2007; Guyenet *et al.* 2008).

However, the idea that involuntary breathing is defined to a very large extent by the excitatory drive that the central pattern generator receives from RTN is only supported by work performed in anaesthetized or neonate rats (Takakura *et al.* 2006; Dubreuil *et al.* 2008). In adult rats, chronic bilateral lesions of the RTN region performed with

---

A. C. Takakura and T. S. Moreira contributed equally to this work.
This paper has online supplemental material.

a saporin-containing toxin attenuate breathing at rest and the activation of breathing by hypercapnia to a similarly modest degree but such lesions do not compromise the survival of the animals (Nattie & Li, 2002; Nattie *et al.* 2004). The authors' interpretation was that the RTN is only one of many sources of pH-regulated excitatory drive to the central respiratory pattern generator of the adult, therefore its elimination is relatively inconsequential (Feldman *et al.* 2003; Nattie & Li, 2006). However, the contribution of the RTN to breathing in the awake state could have been greatly underestimated by these authors if the lesions that they produced had only involved a small portion of the nucleus. This second interpretation should be considered because these authors had no marker to identify the relevant RTN neurons (Nattie & Li, 2002; Nattie *et al.* 2004).

The first objective of the present study was to determine the precise anatomical boundaries of the cluster of $Phox2b^+TH^-$ neurons that seem to be critical with respect to respiratory control. The second objective was to determine whether these cells are effectively and selectively destroyed by a saporin–substance P conjugate (SSP-SAP). The third objective was to determine whether the central chemoreflex is impaired by these lesions in proportion to the degree of destruction of the $Phox2b^+TH^-$ neurons.

We show here that the $Phox2b^+TH^-$ neurons are the predominant neuronal type in the rat RTN and that this nucleus contains about 2100 such neurons spread over a distance of close to 2 mm. We demonstrate that the $Phox2b^+TH^-$ neurons of the RTN are indeed destroyed by SSP-SAP and that the breathing deficit correlates with the percentage loss of these cells. We also suggest that at least 70% of these cells must be eliminated for the apnoea threshold to be substantially elevated under anaesthesia. We conclude that the full contribution of RTN neurons to breathing in unanaesthetized adults is yet to be determined and that this assessment will require the elimination of a much higher proportion of the $Phox2b^+TH^-$ cells than we were able to achieve in the present study.

Methods

The experiments were performed on 51 male Sprague–Dawley rats (Taconic; Germantown, NY, USA) weighing 250–350 g. Procedures were in accordance with NIH Animal Care and Use Guidelines and were approved by the University of Virginia's Animal Care and Use Committee.

Injections of toxin into the retrotrapezoid nucleus

The injections of toxin ([Sar^9,Met(O$_2$)^{11}]-substance P, SSP-SAP (Advanced Targeting Systems, San Diego, CA, USA) were made while the rats were anaesthetized with a mixture of ketamine (75 mg kg^{-1}), xylazine (5 mg kg^{-1})

and acepromazine (1 mg kg^{-1}) administered I.M. Surgery used standard aseptic methods, and after surgery, the rats were treated with the antibiotic ampicillin (100 mg kg^{-1}) and the analgesic ketorolac (0.6 mg kg^{-1}, S.C.). The saporin conjugate was administered into the RTN by pressure injection using glass pipettes with an external tip diameter of 25 μm. These glass pipettes also allowed recordings of field potentials, which were used to direct the electrode tip to the desired sites under the facial motor nucleus. Depending on the experiments, the rats received one injection of toxin into the left RTN, two injections placed symmetrically in the RTN on each side or two pairs of injections placed symmetrically on each side. Each injection was 30 nl. Single injections (unilateral or bilateral) were placed 200 μm below the lower edge of the facial motor nucleus, 1.6–1.9 mm lateral to the midline and 200 μm rostral to the caudal end of the facial motor nucleus. For dual bilateral injections, the first injection was placed at the above described site and the second injection was placed 400 μm rostral to the first one, also 200 μm below the facial motor nucleus. Animals were maintained for 2 weeks before they were used in physiological experiments. The toxin produced no observable behavioural or respiratory effects, regardless of dosage.

The range of doses of SSP-SAP used in the present study (0.15, 0.3 and 0.6 ng (30 nl)$^{-1}$) was selected based on previous experience of the effect of SSP-SAP injected into the pre-Bötzinger complex (Wang *et al.* 2002).

Physiology

General anaesthesia was induced with 5% halothane in 100% oxygen. The rats received a tracheostomy. Artificial ventilation with 1.4–1.5% halothane in 100% oxygen was maintained throughout the surgery. The surgical procedures (femoral artery and vein cannulation, bladder cannulation to ease urination, bilateral vagotomy, phrenic nerve dissection) have been previously described (Guyenet *et al.* 2005; Moreira *et al.* 2006; Takakura *et al.* 2006). In 11 rats both carotid sinus nerves were cut. Upon completion of surgical procedures, halothane was replaced by a mixture of urethane (0.5 g kg^{-1}) and α-chloralose (60 mg kg^{-1}) administered slowly intravenously (I.V.). Rectal temperature was monitored and maintained at 37°C. End-tidal CO$_2$ was monitored throughout the experiment with a capnometer (Columbus Instruments, OH, USA). After injection of the I.V. anaesthetic, the adequacy of anaesthesia was monitored during a 30 min stabilization period by testing for absence of withdrawal response, lack of arterial pressure (AP) change and lack of change in PND rate or amplitude to firm toe pinch. After these criteria were satisfied, the muscle relaxant pancuronium was administered at the initial dose of 1 mg kg^{-1} I.V. and the adequacy of anaesthesia

was thereafter gauged solely by the lack of increase in AP and PND rate or amplitude to firm toe pinch. Approximately hourly supplements of one-third of the initial dose of urethane and chloralose were needed to satisfy these criteria during the course of the recording period (3–4 h). In each rat, the steady-state relationship between integrated PND and end-expiratory CO_2 was determined at the beginning of the experiment and before administration of any supplemental anaesthetic dose in order to minimize the possible impact of the anaesthetic level on these measurements.

All analog data were stored on a computer via a micro1401 digitizer from Cambridge Electronics Design (CED, Cambridge, UK) and were processed off-line using version 5 of the Spike 2 software (CED) as described before (Guyenet *et al.* 2005; Takakura *et al.* 2006). Processing included PND 'integration' (iPND) consisting of rectification and smoothing (τ: 0.015 s) and determination of the total phrenic nerve discharge per unit of time (neural minute × volume, mvPND). mvPND was determined by averaging iPND over 50 consecutive seconds and normalizing the result by assigning a value of 0 to the dependent variable recorded at low levels of end-expiratory CO_2 (below the central apnoeic threshold) and a value of 1 at the highest level of P_{CO_2} investigated (between 9.5 and 10%). Stimulation of carotid chemoreceptors was done with bolus injections of NaCN (50 μg kg^{-1}, i.v.) or by switching the breathing mixture from 100% O_2 to 10–15% O_2 balanced with N_2 for 30 s using an electronic valve. Evidence that the hypoxic stimulus activated neurons via stimulation of carotid chemoreceptors has been previously demonstrated (denervation of these receptors eliminated the excitatory effect of the hypoxic stimulus on PND and the activity of hypoxia-responsive RTN neurons (Takakura *et al.* 2006).

Pharmacological treatments

Muscimol (Sigma Chemical Co.; 1.75 mM in sterile saline pH 7.4) was pressure injected (30 nl) unilaterally through single-barrelled glass pipettes (20 μm tip diameter). The muscimol solution contained a 5% dilution of fluorescent latex microbeads (Lumafluor, New City, NY, USA) for later histological identification of the injection sites (Moreira *et al.* 2006). These injections were made below the facial motor nucleus under electrophysiological guidance as described above (200 μm below the ventral boundary of the facial nucleus, 1.6–1.9 mm lateral to the midline, between Bregma −11.6 and −11.2 mm).

Histology

The rats were deeply anaesthetized with an overdose of urethane (1.8 g kg^{-1}, i.v.) then injected with heparin (500 units, intracardially) and finally perfused through the ascending aorta with 150 ml of phosphate-buffered saline (pH 7.4) followed by 4% phosphate-buffered (0.1 M; pH 7.4) paraformaldehyde (Electron Microscopy Sciences, Fort Washington, PA, USA). The brain was removed and stored in the perfusion fixative for 24–48 h at 4°C. Series of coronal sections (30 μm) from the brain were cut using a vibrating microtome and stored in cryoprotectant solution at −20°C for up to 2 weeks (20% glycerol plus 30% ethylene glycol in 50 mM phosphate buffer, pH 7.4) awaiting histological processing. All histochemical procedures were done using free-floating sections according to previously described protocols (Kang *et al.* 2007). Tyrosine hydroxylase was detected with a mouse antibody (1 : 2000, Chemicon, Temecula) and Phox2b with a rabbit antibody (1 : 800, gift from J.-F. Brunet, Ecole Normale Supérieure, Paris, France). These primary antibodies were detected by incubation with appropriate secondary antibodies tagged with fluorescent reporters to reveal TH (goat anti-mouse Alexa 488, Invitrogen, Carlsbad, CA, USA) and Phox2b (donkey anti-rabbit Cy3, Jackson, West Grove, PA, USA). The substance P receptor (neurokinin 1 receptor, NK1R) was detected using a rabbit NK1R antibody (1 : 5000, Sigma-Aldrich, Saint Louis, MO, USA) raised against a synthetic peptide corresponding to the C-terminal of NK1R of rat origin (amino acids 393–407). Biotinylated donkey anti-rabbit (1 : 500, Jackson) followed by the ABC kit (Vector, Burlingame, CA, USA) and subsequent colourization with 3-3′-di-aminobenzidine (DAB). Choline acetyltransferase (ChAT) was detected with a goat anti-ChAT antibody (1 : 50, Chemicon, raised against human placental ChAT) and revealed with either a fluorescence method using donkey anti-goat Cy3 (1 : 200, Jackson) or the DAB colorimetric method using biotinylated donkey anti-goat (1 : 500, Jackson) and subsequent colourization with DAB. A mouse monoclonal antibody raised against mouse neuronal nuclei (NeuN) 1 : 1000, Chemicon was used as a non-specific neuronal marker and detected with donkey anti-mouse Alexa 488 (1 : 200, Invitrogen). Serotonergic neurons were identified with a mouse monoclonal anti-body against tryptophan hydroxylase (recombinant rabbit protein) (1 : 1000, Sigma) detected with goat anti-mouse IgG$_3$ Alexa 488 (1 : 200, Invitrogen). The specificity of the antibodies has been validated previously (Wang *et al.* 2002; Kang *et al.* 2007).

Cell mapping, cell counting and imaging

Cells were counted using a computer-assisted mapping technique based on the Neurolucida software as previously described (Stornetta & Guyenet, 1999). The Neurolucida files were exported to the NeuroExplorer software (MicroBrightfield, Colchester, VT, USA) to count the

various types of neuronal profiles within a defined area of the reticular formation. When appropriate a selection of the Neurolucida files were also exported to the Canvas 9 software drawing program (ACD Systems of America, Miami, FL, USA) for final modifications.

Section alignment between brains was done relative to a reference section. To align sections around the RTN level, the most caudal section containing an identifiable cluster of facial motor neurons was identified in each brain and assigned the level 11.6 mm caudal to Bregma (Bregma −11.6 mm) according to the atlas of Paxinos & Watson (1998). Levels rostral or caudal to this reference section were determined by adding a distance corresponding to the interval between sections multiplied by the number of intervening sections.

Images were captured with a SensiCam QE 12-bit CCD camera (resolution 1376 × 1040 pixels, Cooke Corp., Auburn Hills, MI, USA). IPLab software (Scanalytics, Rockville, MD, USA) was used for merging of colour channels in photographs of dual labelling experiments.

The neuroanatomical nomenclature is after Paxinos & Watson (1998).

Densitometric analysis of NK1R immunoreactivity

This analysis was conducted in order to assess the regional specificity of the lesions produced by injecting SSP-SAP into the RTN. Images were taken through the region of interest from both sides of the unilateral lesion cases using the same exposure time. The area of interest was outlined using the landmarks as follows. RTN region: at approx. Bregma −11.6 mm, the area was defined by outlining from halfway down the medial edge of the facial motor nucleus around the centre of the ventral edge of this nucleus and then perpendicular to the ventral surface. The region continued medially along the ventral surface to the medial edge of the pyramidal tract and closed with a diagonal to the medial edge of the facial nucleus (see Fig. 3A and B). Note that this region of the brain thus defined encompassed not only the RTN but a large region medial to it. This choice was made because RTN *per se* is not identifiable in tissue reacted for standard NK1R immunochemistry because of the extremely low level of immunoreactivity associated with the Phox2b-expressing neurons (Mulkey *et al.* 2007a). Bötzinger region: at approx. Bregma −11.8 mm, the region was defined by an oval 350 μm wide and 500 μm long, the top centred on the ventral edge of the ambiguus (Fig. 3C). Pre-Bötzinger region: at approx. Bregma −12.6 mm, the region was defined by an oval 350 μm wide and 500 μm long with the top centred on the ventral edge of the ambiguus (Fig. 3D). Rostral ventral respiratory group (rVRG): at approx. Bregma −13.3 mm, the region was defined by an oval 350 μm wide and 500 μm long with the top centred on the ventral edge of the

ambiguus. Using IPLab software (version 3.6, Scanalytics, Rockville, MD, USA) the region was outlined and the region of interest was segmented such that the segments were judged to represent true immunostaining using the nucleus ambiguus as a standard between sections (see Fig. 1 in the online Supplemental material). The area of pixels containing segments was calculated by the software and the data are represented as percentage of control, with control as 100%.

Statistics

Statistical analysis was done with Sigma Stat version 3.0 or 3.1 (Jandel Corporation, Point Richmond, CA, USA). Data are reported as means ± standard error of the mean. One-way parametric ANOVA followed by all pair-wise multiple comparisons (Holm–Sidak method) was used to compare multiple independent treatment groups. Repeated measures (RM) experiments involving more than two measures were analysed by one- or two-way RM ANOVA followed by all pair-wise comparisons (Newman–Keuls method). Significance was set at $P < 0.05$.

Results

Distribution of the Phox2b$^+$TH$^-$ neurons located in the subfacial region of the rostral ventrolateral medulla

In the rostral ventrolateral medulla, Phox2b$^+$TH$^-$ neurons formed a distinctive cluster of very superficial cells that were recognizable by their small, oblong and intensely Phox2b-immunoreactive nuclei (Fig. 1Aa–d). These cells were also easily distinguished from the overlying facial motor neurons the nuclei of which are circular, substantially larger and much less intensely Phox2b-immunoreactive in the adult (Fig. 1Aa). Phox2b$^+$TH$^-$ neurons with oblong and intensely Phox2b-immunoreactive (Phox2b-ir) nuclei were spread out over roughly 2 mm rostrocaudally, from around 400 μm caudal to the facial motor nucleus (Bregma −12.0 mm) to the rostral end of the facial motor nucleus (Bregma −10.0 mm). Because all the Phox2b-ir neurons within this region have very similarly shaped nuclei and form a continous cell group, we considered that all of them belong to the retrotrapezoid nucleus. Caudally, RTN Phox2b$^+$TH$^-$ neurons were in a ventrolateral location relative to the TH$^+$ C1 cell group with minimal overlap of the two cell types (Fig. 1Ab and d). As described before, most C1 cells also expressed Phox2b (Fig. 1Ab–d) (Stornetta *et al.* 2006). The Phox2b$^+$TH$^-$ neurons of the RTN formed two clusters of uneven size. A large and previously described cluster of Phox2b$^+$TH$^-$ neurons
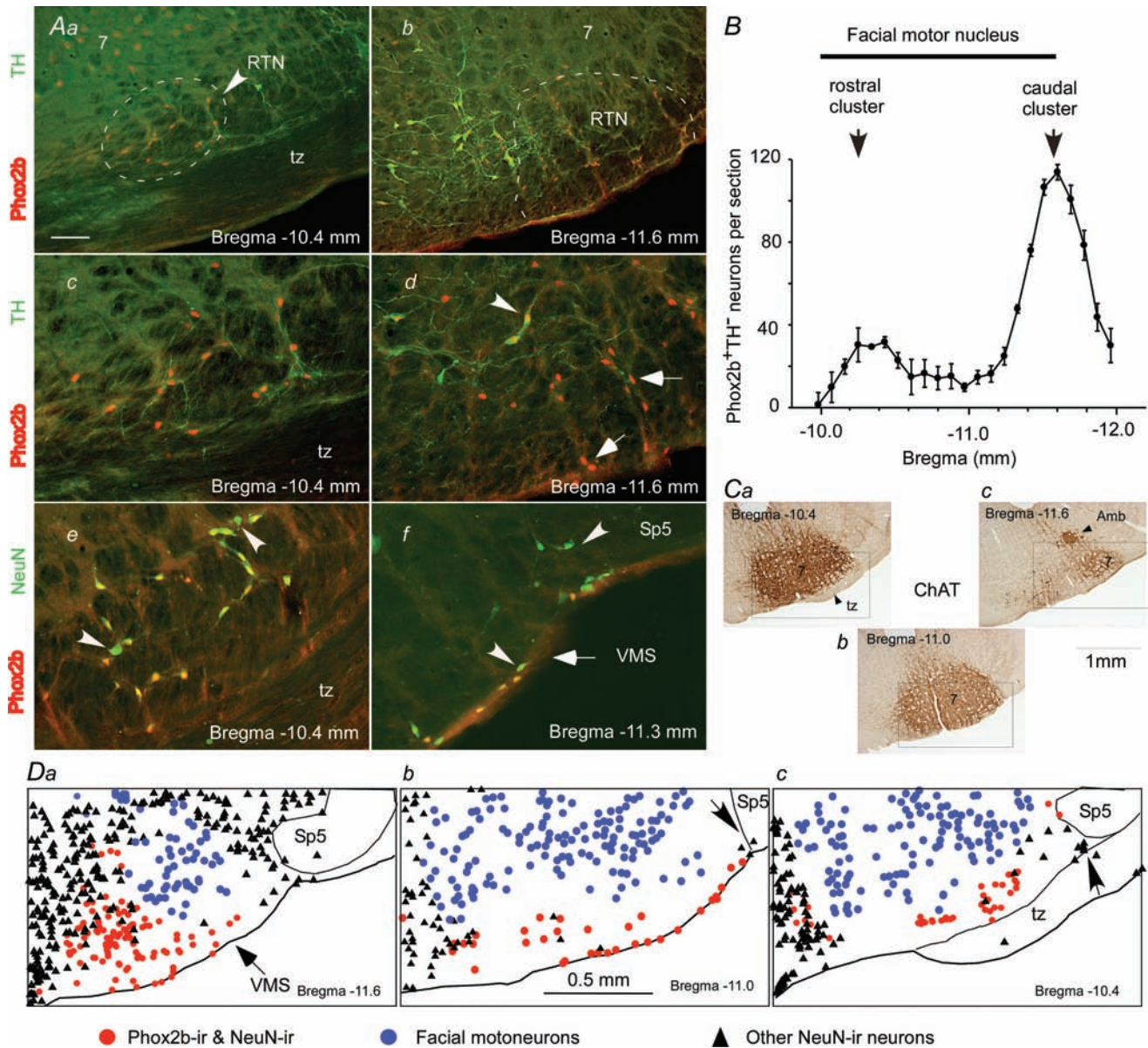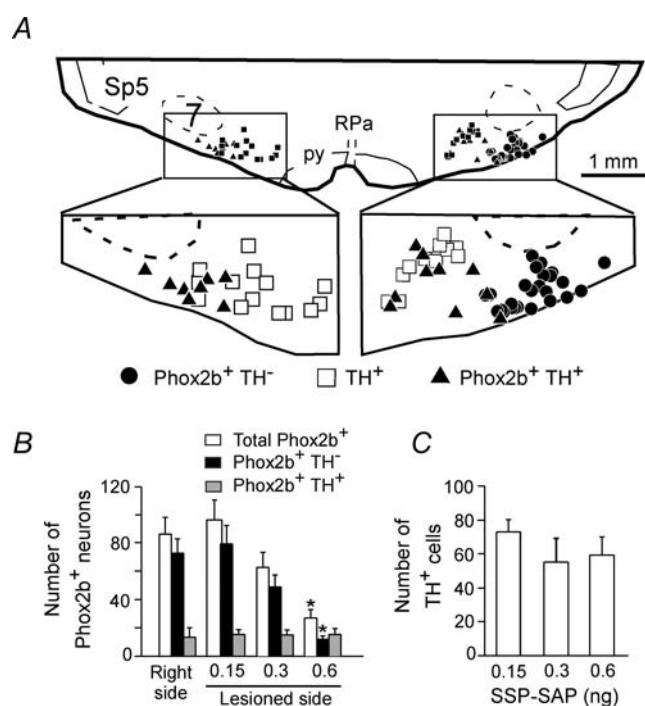
Figure 1. RTN in adult rats

A, photomicrographs of the RTN at two different coronal levels. Phox2b-ir nuclei appear in red (Cy3 fluorescence) and tyrosine hydroxylase (TH) in green (Alexa 488 fluorescence). *Aa* and *Ac* depict the rostral cluster of Phox2b$^+$TH$^-$ neurons at two magnifications (tz, trapezoid body; 7, facial motonucleus). *Ab* and *Ad* show the much larger caudal cluster, also at two magnifications. *Ae* shows that all the NeuN-immunoreactive neurons located in this field except two (indicated by arrowheads) express Phox2b. *Af* shows the small cluster of Phox2b-negative neurons located at the lateral edge of RTN next to the spinal trigeminal tract (Sp5). *B*, rostrocaudal distribution of the Phox2b$^+$TH$^-$ neurons. Cell counts were obtained from a one-in-three series of 30 μm-thick coronal sections from 6 intact rats. Section alignment was done using as reference the coronal section closest to the caudal end of the facial motor nucleus in each brain (this level is indicated in the choline acetyl-transferase-stained section shown in *Cc*. The ordinate indicates the number of neurons detected on both sides. *Ca–c* are coronal sections immunostained for choline acetyl-transferase. *Da–c* are computer-assisted plots of the location of three types of cells identified in sections reacted for NeuN and Phox2b. Facial motoneurons were identified by their large size and weakly Phox2b-ir nuclei. The black triangles represent all the NeuN-ir neuronal nuclei that do not belong to the other two neuronal categories. The red circles indicate both C1 cells and the presumed chemoreceptors. The calibration bar in *Aa* represents 100 μm in panels *Aa*, *Ab* and *Af*. This bar represents 50 μm in *Ac*, *Ad* and *Ae*. Bregma levels are according to the atlas of Paxinos & Watson (1998). VMS = ventral medullary surface

A. C. Takakura and others

(Stornetta *et al.* 2006) is centred at the caudal end of the facial motor nucleus (Bregma −11.6 mm; Fig. 1*Ab*, *B* and *Cc*). A second cluster of Phox2b$^+$TH$^-$ neurons is centred approximately at Bregma −10.4 mm below the facial motor nucleus and just above the medial tip of the trapezoid body (Fig. 1*Aa* and *c*, *B* and *Ca*). The region located between these two clusters contained many fewer Phox2b$^+$TH$^-$ cells, sometimes no more than 2–5 cells per side and most of these neurons were located at the ventral surface of the medulla within the marginal layer (Fig. 1*Db*). In this intermediate region, the dendrites of the facial motoneurons occupy virtually all the space located between their cell bodies and the ventral medullary surface (Fig. 1*Cb* and *Db*). The rostrocaudal distribution of the Phox2b$^+$TH$^-$ cells that reside under the facial motor nucleus is shown in Fig. 1*B* (average of 6 rats). The total number of nuclei found in every third section was 868 ± 29 per rat. The Abercrombie correction (Abercrombie, 1946; Williams & Rakic, 1988) was used to obtain an estimate of the total number of Phox2b$^+$TH$^-$ neurons of the RTN. The correction factor was based on the average diameter of the nucleus in the coronal plane (7 ± 0.2 μm) and the

section thickness measured at 30 μm without dehydration. The nuclei of the Phox2b$^+$TH$^-$ neurons are oval with the long axis in the coronal plane; therefore their rostrocaudal dimension should be roughly the same as the length of the shorter axis in the coronal plane. Based on these values and assumptions, the total calculated number of Phox2b$^+$TH$^-$ cells was 2112 ± 71 neurons per brain ($n = 6$).

In three rats, a one-in-six series of coronal sections was reacted for simultaneous detection of the pan-neuronal marker NeuN and Phox2b. This experiment was done to determine whether the region located below the facial motor nucleus contains neurons that do not express Phox2b. As shown in Fig. 1*Ae* and *Da–c*, NeuN-ir neurons devoid of a Phox2b-ir nucleus were extremely rare in this region except at its lateral margin where a small cluster of 1–5 Phox2b-negative neurons per section was generally present in close proximity of the ventral surface just medial to spinal trigeminal tract (Fig. 1*Af*, and *Db* and *c*). Because the medial edge of the RTN overlaps with a region of the medulla that has a very high neuronal density (Fig. 1*Da–c*) the exact border of the nucleus is difficult to define. For this reason, we did not attempt to quantify the proportion of Phox2b-negative neurons located within this nucleus. However, inspection of 12 representative sections from three rats (examples in Fig. 1*D*) suggests that the region located under the lateral two-thirds of the facial motor nucleus has a very low neuronal density and that over 90% of the NeuN-positive neurons present in this region have intensely Phox2b-ir cell bodies with a shape characteristic of RTN neurons.

## SSP-SAP destroys selectively the Phox2b$^+$TH$^-$ neurons of RTN

SSP-SAP (single 30 nl microinjection containing 0.15, 0.3 or 0.6 ng of toxin; MW 33 000) was administered into the left RTN in three groups of rats in order to determine the most effective dose of toxin and the specificity of the lesion. Phox2b and TH immunoreactivities were examined within the RTN region in all the SSP-SAP-injected rats to assess the effect of the toxin on the Phox2b$^+$TH$^-$ neurons and on the nearby catecholaminergic neurons. Phox2b$^+$TH$^-$ and TH$^+$ neurons with or without Phox2b were plotted and counted in nine coronal sections per rat. Each section was 180 μm apart and the mid-section was selected to coincide with the caudal end of the facial motor nucleus. Figure 2*A* is a representative plot from a rat that had received a 0.6 ng dose of SSP-SAP on the left side. Phox2b$^+$TH$^-$ neurons were absent from the left side but the number of TH$^+$ neurons was approximately the same on both sides. Group data (Fig. 2*B* and *C*) indicated that the 0.15 ng dose of toxin was ineffective and the 0.3 ng dose marginally effective (no statistical difference by ANOVA). The 0.6 ng dose of toxin reduced

Figure 2. SSP-SAP destroys Phox2b$^+$TH$^-$ neurons selectively
A, computer-assisted plot of the Phox2b$^+$TH$^-$ neurons and C1 neurons (TH$^+$) present in a single 3 μm-thick coronal brain section from a rat that had received a single 0.6 ng dose of SSP-SAP on the left side of the brain (Bregma level around −11.6 mm). Note the selective loss of the Phox2b$^+$TH$^-$ neurons on the side with the lesion. *B* and *C*, group data. Each column represents the total number of neurons of a given type present in 9 consecutive 30 μm-thick coronal sections separated by 180 μm. The middle section was as close as possible to Bregma −11.6 mm. RPa = raphe pallidus, py = pyramidal tract.

the number of Phox2b$^+$TH$^-$ neurons counted in the nine sections by $85 \pm 3\%$ without significant decrease in the number of TH$^+$ neurons (Fig. 2*B* and *C*). The fraction of catecholaminergic neurons that expressed detectable levels of Phox2b was also unaffected by the toxin (Fig. 2*A* and *B*). This observation indicates that 0.6 ng of SSP-SAP selectively killed the Phox2b$^+$TH$^-$ neurons. The resistance of TH$^+$ neurons to SSP-SAP is consistent with previous observations (Gray *et al.* 2001; Wang *et al.* 2002).

To further assess the selectivity of the lesions, we systematically examined the intensity of the NK1R immunoreactivity present within four consecutive segments of the ventral respiratory column namely the RTN, the Bötzinger region (BötC), the pre-Bötzinger complex (preBötC) and the rostral ventral respiratory group (rVRG). The 0.15 ng dose of SSP-SAP produced no detectable lesion in any region (the RTN level is shown in Fig. 3*Aa* and *b*, and *E*). The 0.3 ng dose produced a small reduction in NK1R immunoreactivity in the RTN region which failed to reach statistical significance at the group level (Fig. 3*E*). The rats that received 0.6 ng SSP-SAP had extensive unilateral reductions of NK1R immunoreactivity within the RTN region and medial to it (Fig. 3*Ba* and *b*, and *E*; lesion side: $10 \pm 4\%$ of contralateral side) and a small but significant reduction within the BötC, the region of the ventral respiratory column closest to RTN (Fig. 3*Ca* and *b*,

and *E*; lesion side: $67 \pm 9\%$ of control side; $P < 0.05$). No change of NK1R immunoreactivity was detected further caudally within the ventral respiratory column (Fig. 3*Da* and *b*, and *E*; preBötC lesion side: $101 \pm 8\%$ of control side, not significant (n.s.); rVRG lesion side: $111 \pm 8\%$ of control side, n.s.).

To further assess the selectivity of the toxin we examined the effect of 0.6 ng SSP-SAP on specific types of neurons located in the immediate proximity of RTN. Based on choline-acetyltransferase (ChAT) immunoreactivity, the toxin had no detectable effect on facial motor neurons nor on the small ChAT-ir neurons located between RTN and the edge of the pyramidal tract (Fig. 2 in Supplemental material). The nucleus ambiguus was also spared, presumably because of its physical distance from the SSP-SAP injection site rather than by a lack of sensitivity to the toxin given that this nucleus expresses extremely high levels of NK1Rs (Fig. 3*A*, *B* and *C*). Based on the examination of sections stained with an antibody against tryptophan hydroxylase, 0.6 ng SSP-SAP had no obvious effect either on the serotonergic neurons, including those located closest to RTN, i.e. at the lateral edge of the pyramids (Fig. 2 in Supplemental material). However, the toxin did destroy a group of large and strongly NK1R-ir neurons also located at the lateral edge of the pyramidal tract (Fig. 3*Ba* and *b*). As noted by previous investigators, these neurons
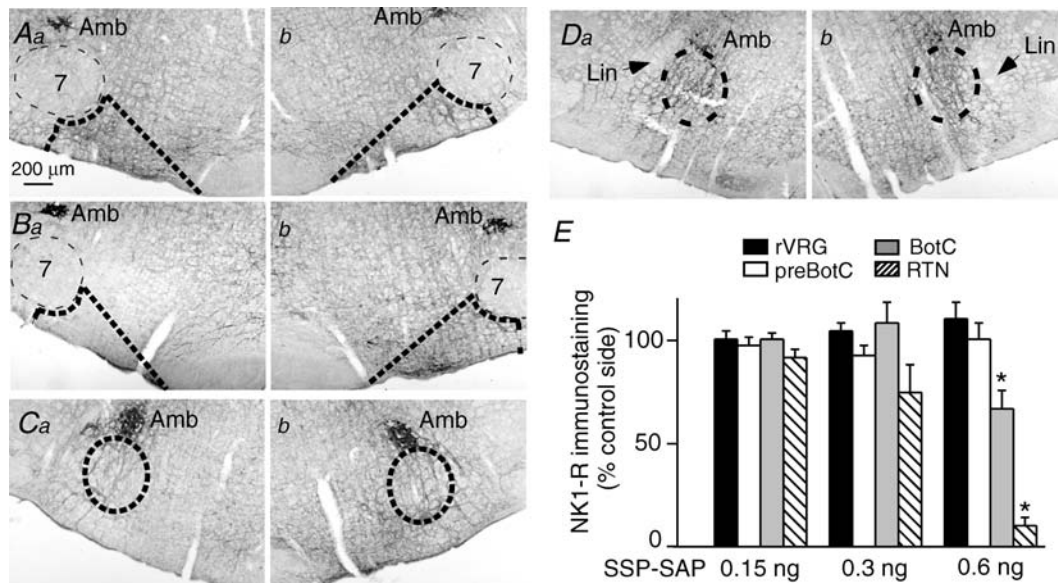
Figure 3. Effect of SSP-SAP on NK1 receptor immunoreactivity
Aa and *b*, injection of 0.15 ng of SSP-SAP into the left RTN (*a*) produced no effect on NK1R immunoreactivity (*b* control side; coronal sections at Bregma −11.6 mm). *Ba* and *b*, injection of 0.6 ng of SSP-SAP into the left RTN virtually eliminated NK1R immunoreactivity (*Ba*). The opposite side (*Bb*) was intact. *Ca* and *b*, injection of 0.6 ng of SSP-SAP into the left RTN slightly reduced NK1R immunoreactivity in the Bötzinger region identified by the ellipse (*Ca*). The opposite side (*Cb*) was intact. *Da* and *b*, injection of 0.6 ng of SSP-SAP into the left RTN had no effect at the level of the pre-Bötzinger complex identified by the ellipse (*Da* injected side; *Db* opposite side). *E*, analysis of the extent of NK1R immunoreactivity in the regions outlined by the dotted lines in *Aa–Db*. NK1R immunoreactivity on the side with the lesion is expressed as percentage control of the immunoreactivity on the intact side. * Statistical difference from the control side by RM ANOVA. Lin = nucleus linearis.
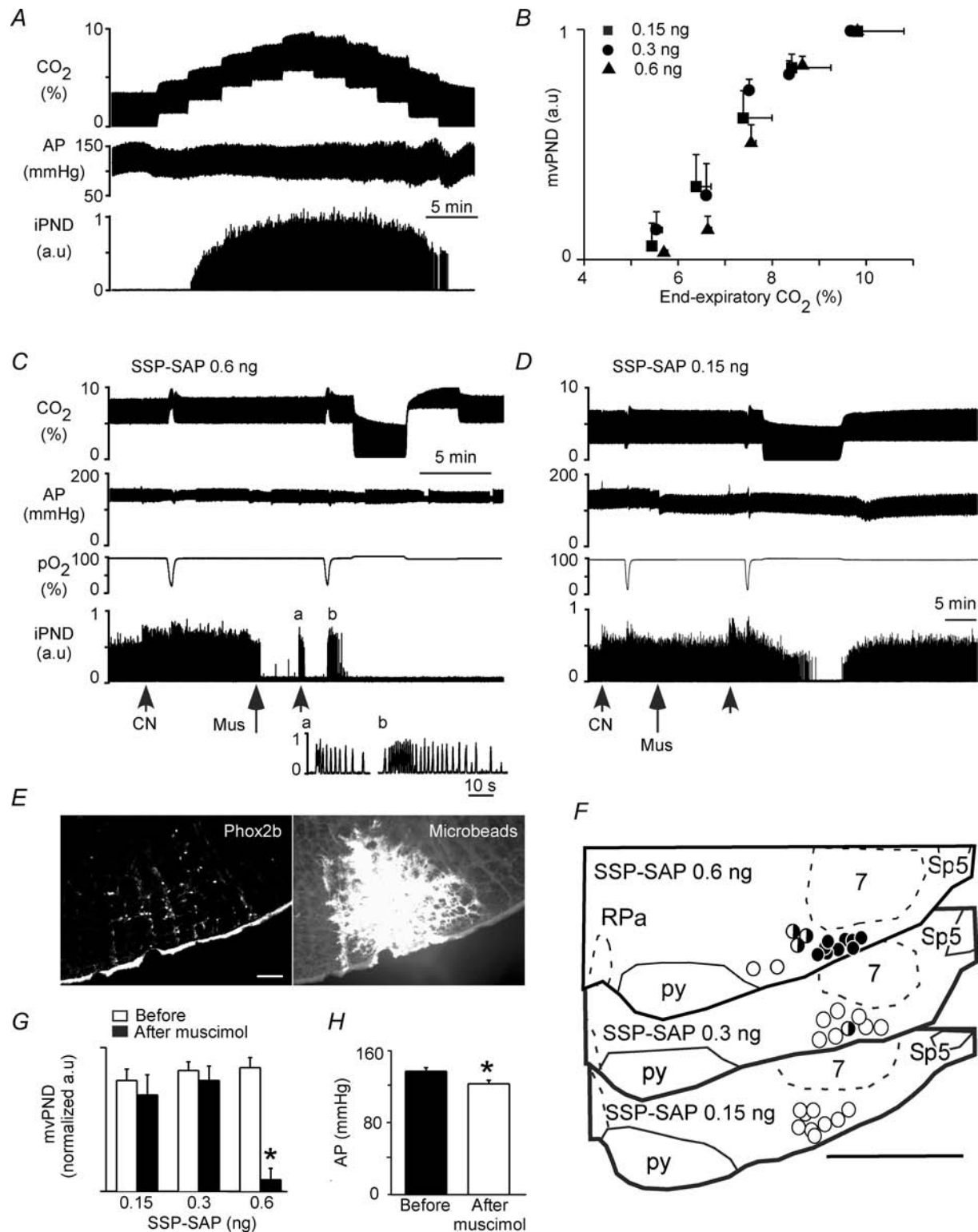
Figure 4. Muscimol injection into the intact RTN eliminates phrenic nerve discharge (PND) in rats with a contralateral lesion

A, relationship between iPND and end-expiratory CO_2 at steady state (rat with injection of ineffective dose of SSP-SAP, 0.15 ng). *B*, relationship between mvPND and end-expiratory CO_2 at steady state in groups of rats treated with 0.15 ng ($n = 9$), 0.3 ng ($n = 8$) or 0.6 ng SSP-SAP ($n = 14$). Note that none of the lesions caused a significant rise in the apnoeic threshold. *C*, injection of muscimol (52 pmol $(30 \text{ nl})^{-1}$) into the right RTN of a rat injected 2 weeks previously with 0.6 ng SSP-SAP in the left RTN eliminated PND instantly. PND with normal

have dendrites that extend well into the RTN region (Nattie *et al.* 2004). The destruction of these dendrites by SSP-SAP probably accounts for a large percentage of the overall decrease in NK1R immunoreactivity caused by SSP-SAP within the RTN region since, as noted before, the NK1R immunoreactivity associated with the cell bodies of the Phox2b-expressing RTN neurons is extremely weak (Mulkey *et al.* 2007*a*).

Effects of unilateral destruction of the RTN neurons on PND and central respiratory chemosensitivity

Prior to histology, the three groups of rats described in the previous paragraph were also subjected to physiological experiments under anaesthesia. We first determined whether the steady-state relationship between PND and end-expiratory CO_2 was altered in these rats and found no change regardless of the toxin dose (Fig. 4*A* and *B*). A slight increase in CO_2 threshold may have occurred at the highest toxin dose (0.6 ng, Fig. 4*B*) but the difference was not statistically significant. Because the 0.6 ng dose of toxin destroyed 85% of the caudal cluster of Phox2b$^+$TH$^-$ neurons on one side but left the rostral cluster intact, it can be estimated that the side with the lesion still contained approximately 32% of its normal complement of Phox2b$^+$TH$^-$ neurons and that two-thirds of the total number of Phox2b$^+$TH$^-$ neurons of the RTN were still intact in these rats.

Next, we determined the effects of silencing the right intact RTN with muscimol (1.75 mm, 30 nl) on PND at rest and during hypercapnia (up to 10% end-expiratory CO_2). The 'muscimol test' was performed in rats that had been treated 2 weeks before with, respectively, 0.15 ($n = 9$), 0.3 ($n = 8$) or 0.6 ng SSP-SAP ($n = 14$) on the left side. The tips of the muscimol-containing pipettes were inserted under electrophysiological guidance, typically 250 μm below the facial motor nucleus and 200 μm rostral to the caudal end of this nucleus to target the caudal cluster of Phox2b$^+$TH$^-$ neurons. The accuracy of the injection sites was verified *post hoc* by examining the location of the fluorescent microbeads incorporated into the injected solution. In the 0.6 ng group ($n = 12$) muscimol injections placed accurately into the surviving RTN eliminated resting PND

(example in Fig. 4*C*). The inhibition was instantaneous when muscimol was injected accurately into the RTN as judged by the coincidence between the fluorescent microbeads and the cluster of Phox2b$^+$TH$^-$ neurons (9 of 14 cases; Fig. 4*E*). This site and the other eight accurate muscimol placements are depicted by black circles in Fig. 4*F*. PND inhibition was delayed by 1–3 min when muscimol was injected slightly medial to the RTN (3 out of 14 rats; black and white circles in Fig. 4*F*). In each of these 12 cases PND inhibition was complete and, in all but two, PND could not be restored by elevating end-expiratory CO_2 up to 10% (e.g. Fig. 4*A*). PND inhibition lasted for a minimum of 1 h (not illustrated). The two cases in which some PND could be restored by raising CO_2 corresponded to an injection of muscimol placed slightly medial to RTN (2 of the 3 cases identified by black and white circles in Fig. 4*F*, upper section). However, in most cases (8/12, including 6 of the 10 cases in which PND could not be reactivated to any extent by hypercapnia) phasic and apparently normal PND could be transiently elicited by stimulating peripheral chemoreceptors with hypoxia or intravenous cyanide (Fig. 4*C*, insets a and b). Thus, in most instances in which a muscimol injection eventually eliminated resting PND (8/12 rats), we obtained evidence that the respiratory oscillator was still functional because phasic and seemingly normal PND could be elicited by stimulating peripheral chemoreceptors with hypoxia or cyanide. In 2 of the 14 rats with a 0.6 ng SSP-SAP lesion of the contralateral RTN, muscimol injection into the side without a lesion had no effect on inspiratory activity. Upon histological inspection, the muscimol injection sites were found at the lateral edge of the pyramidal tract about 700 μm medial relative to the centre of RTN (open circles in Fig. 4*F*, upper section).

In rats treated with 0.15 ng SSP-SAP ($n = 8$), a unilateral injection of muscimol into the RTN on the side contralateral to the toxin injection site had no effect on resting PND in any of the rats (Fig. 4*D* and *G*) although the injection sites were properly placed (Fig. 4*F*, lower section, open circles). In the 0.3 ng group ($n = 8$), unilateral muscimol injection into RTN on the side contralateral to the SSP-SAP injection generally had no effect on resting PND either (Fig. 4*F*, middle section, open circles) except in

characteristics could be transiently restored by peripheral chemoreceptor stimulation (a, cyanide; b, brief hypoxia). PND could not be restored by increasing end-expiratory CO_2 up to 10% (right portion of recording). D, injection of the same amount of muscimol (52 pmol (30 nl)$^{-1}$) into the right RTN of a rat injected 2 weeks previously with 0.15 ng SSP-SAP in the left RTN produced no effect. E, example of a muscimol injection centred in the caudal cluster of Phox2b$^+$TH$^-$ neurons (left, Phox2b immunoreactivity, Cy3; right, fluorescein-tagged microbeads delineating the area that was exposed to muscimol). This injection site produced the effect shown in C. F, summary of muscimol injection sites performed in groups of rats treated on the left side with 0.6 ng of SSP-SAP (top section), 0.3 ng (middle section) and 0.15 ng of toxin (lower section). G, group data showing the effect of muscimol on resting PND in the three groups of rats with toxin injections. PND normalization (1 arbitrary unit) represents the maximum PND activity registered during steady state at 10% end-expiratory CO_2 in pure oxygen (*$P < 0.05$ by RM ANOVA). H, effect of muscimol on resting blood pressure in the 0.6 ng treatment group.

Table 1. Summary of the experiments performed in rats subjected to unilateral injections of SSP-SAP into RTN

SSP–SAP (dose)	n (rats)	Resting PND reduced	No PND at rest	PND recovery at 10% CO_2	Phasic PND inducible by hypoxia or cyanide
0.6 ng	12	0	12	2	8
0.3 ng	8	1	0	8	8
0.15 ng	9	0	0	9	9

At rest, end-expiratory CO_2 was set at 6.5–7%, the level at which the phrenic nerve discharge (PND) reached 50–75% of its maximum amplitude. Columns 3–6 summarize the effects produced by a single injection of muscimol into the RTN on the side contralateral to a lesion produced by injecting SSP-SAP at each of the three doses indicated in column 1.

one case (black and white circle in Fig. 4*F*). In this animal, resting PND was only partially reduced by muscimol and PND could be further activated by hypercapnia (10%). On average, a muscimol injection placed into or very close to the intact RTN eliminated resting PND only in the group of rats treated with the 0.6 ng dose of toxin (12/14 rats). For added clarity, Table 1 summarizes the outcome of the muscimol experiments done in the three groups of rats.

The muscimol injections also slightly reduced blood pressure (BP). The BP reduction was slightly greater in the 0.6 ng SSP-SAP group (123 ± 3 mmHg after muscimol from a resting value of 144 ± 3 mmHg) than in the other two groups (0.3 ng group: 133 ± 4 mmHg after muscimol from a resting value of 144 ± 5 mmHg; 0.15 ng group: 129 ± 3 mmHg after muscimol from a resting value of 136 ± 2 mmHg). The BP drop observed in the 0.6 ng group was significantly greater than that observed in the other two groups ($P < 0.05$ by ANOVA). Resting blood pressures were statistically the same in all groups and muscimol produced the same hypotension in the groups treated with the two lowest doses of toxin.

Impairment of central chemoreflex correlates with loss of Phox2b$^+$TH$^-$ neurons after bilateral lesions of RTN with SSP-SAP

In one group of six rats 0.6 ng SSP-SAP was injected on each side of the brain into the RTN at the level of the caudal end of the facial motor nucleus (Bregma −11.6 mm). A second group of rats ($n = 11$) received two injections of 0.6 ng SSP-SAP on each side of the brain (total of four injections). The caudalmost injections were also aimed at Bregma −11.6 mm under the facial motor nucleus and the others were placed 400 μm rostral to the first ones, also under the facial motor nucleus. All the animals survived the procedure without apparent harm and grew at a normal rate. Two weeks later, the animals were anaesthetized and

the central chemoreflex was determined by testing the relationship between PND and end-expiratory CO_2 at steady state as shown in Fig. 5. The apnoeic threshold was quantified and compared to that of 19 control rats. The control population included the previously described rats treated unilaterally with an ineffective dose of toxin (0.15 ng or 0.3 ng; $n = 16$) and three rats that had been injected bilaterally at two sites with saline instead of SSP-SAP. The former group had intact carotid sinus nerves and these nerves were cut in the latter three rats. The presence or absence of the carotid sinus nerves had no effect on the apnoeic CO_2 threshold presumably because the balance of respiratory gases consisted of pure oxygen. The residual number of Phox2b$^+$TH$^-$ neurons present throughout the entire length of the RTN was determined in the rats with toxin injections and was compared to the cell counts from six control rats (3 uninjected rats and 3 rats injected bilaterally with saline).

The apnoeic threshold of the rats that had received two injections of toxin on each side ($n = 11$) was markedly elevated relative to the control rats ($7.9 \pm 0.3\%$ end-expiratory CO_2 *versus* $5.6 \pm 0.2\%$, $P < 0.05$; Fig. 5*B*, *C* and *D*). In this group of rats, the number of surviving RTN Phox2b$^+$TH$^-$ neurons was $30 \pm 3.5\%$ of control (range 15–54%; $n = 10$, one rat was not processed for histology for technical reasons). The apnoeic threshold of the rats that had received only one injection of SSP-SAP per side was slightly higher than that of the control group ($6.4 \pm 0.3\%$ end-expiratory CO_2 *versus* $5.6 \pm 0.2\%$), but the difference was not statistically significant by ANOVA (Fig. 5*D*). In this second group the number of surviving RTN Phox2b$^+$TH$^-$ neurons was $43 \pm 3\%$ of control (range 35–55%; $n = 6$). This percentage was significantly greater than in the rats that had receive two injections of toxin per side ($P = 0.027$ by *t* test). In addition the apnoeic threshold was inversely correlated with the number of surviving Phox2b$^+$TH$^-$ neurons when both groups of lesioned rats (the two-injection and the four-injection groups) were considered together ($n = 15$ cells; Fig. 5*E*).

The relationship between the elevation of the apnoeic threshold and the loss of the Phox2b$^+$TH$^-$ neurons was non-linear as suggested by a comparison of the two bilaterally lesioned groups with the unlesioned control (Fig. 5D). In all cases, including the group that had received four injections, the rostral cluster of Phox2b$^+$TH$^-$ neurons was spared (Fig. 6).

Discussion

This study updates the anatomical boundaries of a group of Phox2b$^+$TH$^-$ neurons suspected to underlie the stimulatory role of the RTN in breathing. We show

that these neurons are selectively but not specifically destroyed when the toxin SSP-SAP is injected in their midst. We also show that the acute inhibition or the chronic loss of the Phox2b$^+$TH$^-$ cells causes a substantial elevation of the apnoeic threshold. These results extend previous evidence that the RTN region up-regulates breathing and the central chemoreflex. Consistent with the known cellular properties of Phox2b$^+$TH$^-$ neurons and with recent evidence that the genetic deletion of these cells eliminates the chemoreflex at birth, the present results suggest that these RTN neurons contribute a CO_2-modulated excitatory drive to the breathing network that may be essential for CO_2 stability *in vivo*.
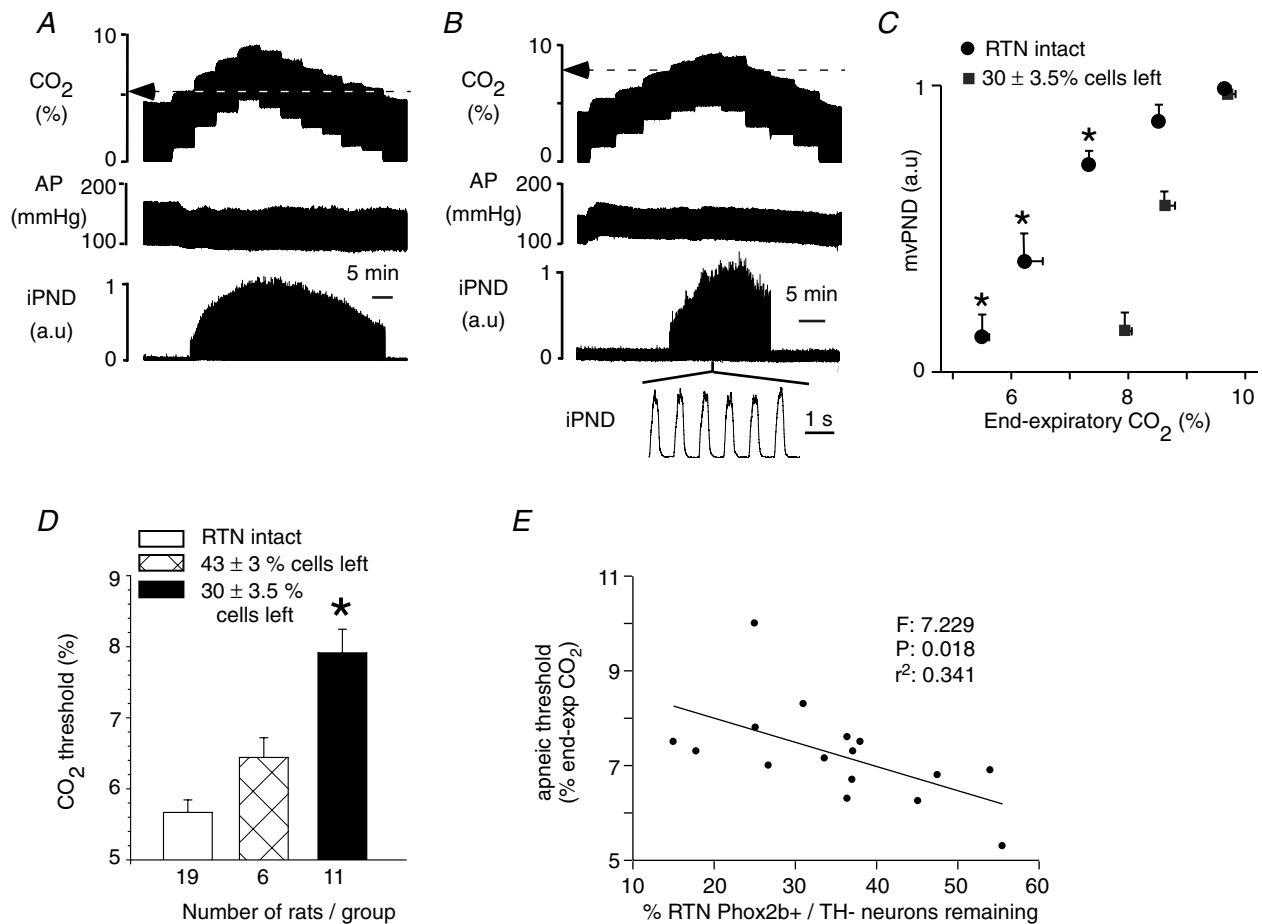
Figure 5. Effect of bilateral injections of SSP-SAP into the RTN on the central chemoreflex
A, relationship between PND and end-expiratory CO_2 in a control rat 2 weeks after bilateral injection of saline. The apnoeic threshold is 5.2%. B, same experiment in a different rat 2 weeks after bilateral treatment with 2×0.6 ng of SSP-SAP. The apnoeic threshold is 7.9%. PND above the apnoeic threshold appears normal. C, relationship between mvPND and end-expiratory CO_2 in controls ($n = 19$) and in 11 rats treated bilaterally with 2×0.6 ng of SSP-SAP causing the destruction of 70% of the Phox2b$^+$TH$^-$ neurons of RTN. One arbitrary unit represents the highest value of mvPND registered at steady state with end-expiratory CO_2 set at 9.5–10%. * Statistical significance by RM ANOVA ($P < 0.05$). D, effect of graded lesions of the Phox2b$^+$TH$^-$ neurons of the RTN on the apnoeic threshold measured as shown in A and B. * Statistically significant difference from the other two groups by ANOVA ($P < 0.05$). E, correlation between apnoeic threshold and percentage Phox2b$^+$TH$^-$ neurons remaining (10 rats with 2 injections of toxin on each side and 6 rats with one injection on each side). The F, r^2 and probability values of the linear regression are indicated in the figure.

Updating the definition of the RTN

Brain nuclei are defined as collections of neurons that share specific anatomical or biochemical characteristics and are located within a defined and limited region of the brain. Applying these general principles we updated our previous definition of the RTN to include a large rostral extension of this structure. The present definition of RTN neurons is based on anatomical considerations, specifically the small usually oblong shape of the nucleus of these cells, their intense Phox2b immunoreactivity and the absence of tyrosine hydroxylase. These criteria

clearly distinguish these cells from the neighbouring C1 adrenergic neurons and from the overlying facial motoneurons. Every Phox2b-ir cell nucleus contained the neuronal specific marker NeuN demonstrating that, within this region, Phox2b is expressed exclusively by neurons.

We have previously shown that the caudal portion of the RTN contains neurons that are strongly activated by CO_2 and that these neurons are $Phox2b^+TH^-$ and glutamatergic (Stornetta *et al.* 2006). We have also demonstrated that neurons selected from this region of
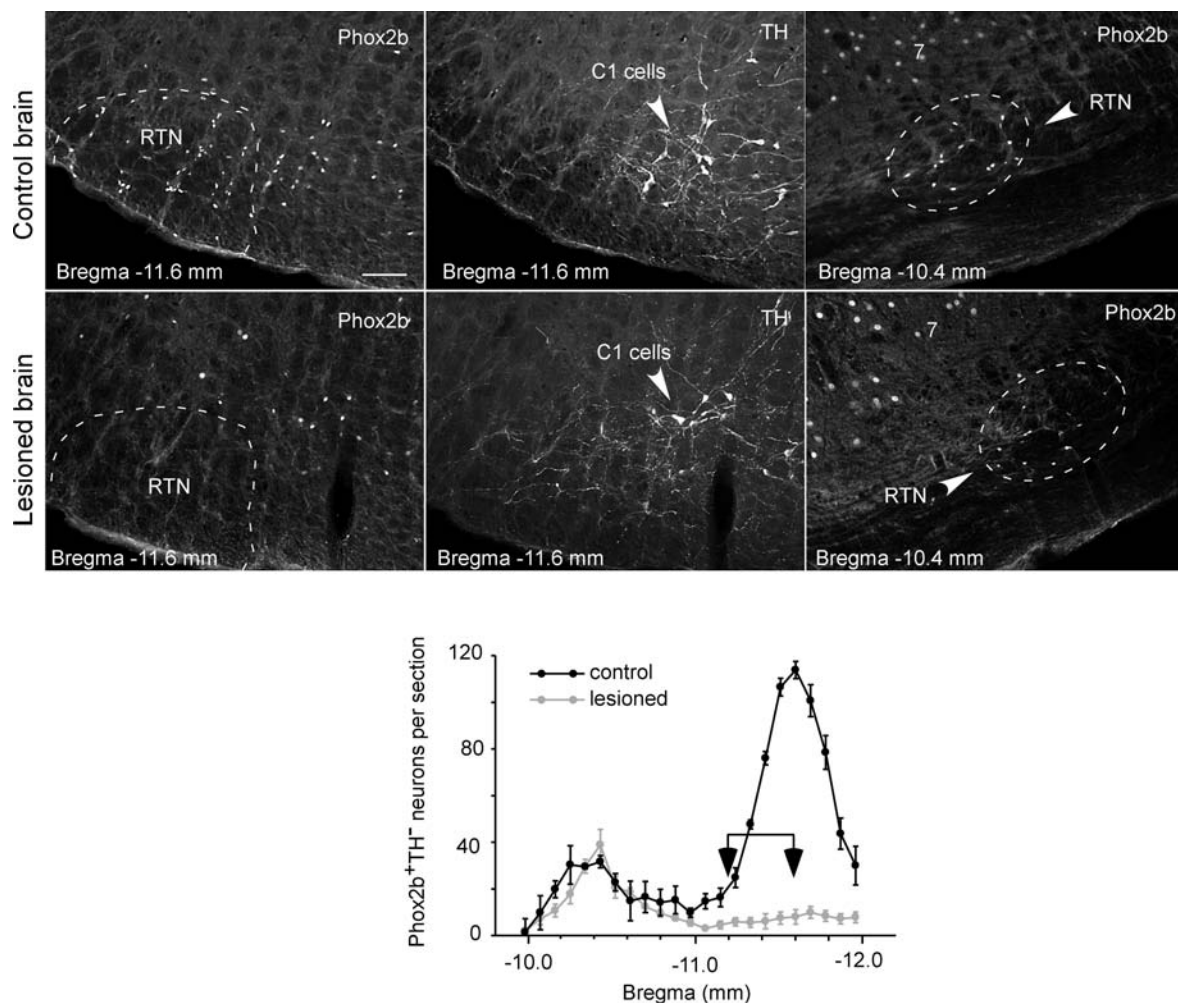
Figure 6. Effect of bilateral injections of SSP-SAP on RTN neurons
The top row of photomicrographs is from a control rat that received 4 injections of saline. The lower row is from a rat that received two injections of 0.6 ng SSP-SAP in the RTN on each side. The left column demonstrates the almost complete loss of the $Phox2b^+$ nuclei (Cy3 immunofluorescence) at the level of the caudal cluster of the RTN (Bregma level −11.6 mm). The middle panels show the C1 neurons present in the same fields (TH immunoreactivity, Alexa 488). Note that most of the few remaining $Phox2b^+$ nuclei belong to C1 neurons. The right column shows that the rostral cluster of $Phox2b^+$ neurons was still intact in the toxin-treated RTN. Calibration bar in top left panel (100 μm) applies to all panels. The graph at the bottom compares the distribution of the $Phox2b^+TH^-$ neurons throughout the RTN in 11 rats with bilateral lesions (grey) to the cell distribution found in 6 control rats (re-plot of the graph already shown in Fig. 1). The arrows indicate where the two injections of 0.6 ng of SSP-SAP were placed on each side.

the brain in slices on the basis of their acid-sensitivity have the same biochemical characteristics (Mulkey *et al.* 2007*b*). Based on this and other considerations we have proposed that the Phox2b$^+$TH$^-$ neurons are central respiratory chemoreceptors.

Judging from the present study, we would argue that, in the adult rat, there are very few neurons under the lateral two-thirds of the facial motor nucleus besides the Phox2b$^+$TH$^-$ ones and a very small group of neurons located at the medial margin of the trigeminal tract (Fig. 1*Af*, and *Db* and *c*). A possible loophole in this reasoning would be that the region located under the lateral two-thirds of the facial motor nucleus contains a substantial group of neurons that we missed because they do not express the antigen recognized by the NeuN antibody. Although such neurons exist elsewhere (Purkinje neurons, mitral cells and photoreceptors), this interpretation is unlikely because inspection of sections stained with cresyl violet confirm the impression that the region that lies under the facial motor nucleus is extremely neuronally poor.

Other investigators have postulated that the lateral and anterior subfacial region contains rhythmogenic neurons implicated in the generation of inspiratory or expiratory activity (Onimaru & Homma, 2003; Onimaru *et al.* 2006; Feldman & Del Negro, 2006). These neurons are called the parafacial respiratory group or pfRG. Until the biochemical signatures of the pfRG neurons are revealed, it will be difficult to establish their relation with the RTN neurons that we have defined as chemoreceptors in the adult but the present study suggests several possibilities. Although we have demonstrated that the CO_2/pH-sensitive neurons of the RTN region are Phox2b$^+$TH$^-$, we have not proven the converse. It is therefore possible that a subset of the Phox2b$^+$TH$^-$ neurons have pfRG-like discharge characteristics in the neonate brainstem *in vitro*, the preparation in which such cells have been recorded (Onimaru & Homma, 2003). It is also conceivable that the pfRG neurons migrate laterally during the early postnatal period to become the lateral group of superficial Phox2b-negative neurons identified here. Finally, it is also possible that the properties and or connectivity of the caudal and rostral clusters of Phox2b$^+$TH$^-$ neurons might be different. For example, the rostral cluster might conceivably play a preferential role in regulating expiratory activity (Janczewski & Feldman, 2006; Feldman & Del Negro, 2006; Taccola *et al.* 2007) whereas the caudal cluster might regulate inspiratory activity preferentially (Onimaru & Homma, 2003). However, given the highly speculative nature of these possibilities, in the rest of the discussion, we will assume that the properties and role of the Phox2b$^+$TH$^-$ cells are the same everywhere and that these properties are those that have already been identified *in vivo* and *in vitro* in the adult rat (Mulkey *et al.* 2004; Guyenet *et al.* 2008).

Deficits caused by RTN lesions or by injecting muscimol in RTN: comparison with previous studies

Under our experimental conditions, unilateral injection of muscimol into the RTN produced no effect on the PND. In awake rats, application of muscimol with a dialysis probe into a similar region decreased tidal volume (V_T) slightly although ventilation ($\dot{V}_E$) was only transiently reduced due to an increase in breathing frequency (Nattie & Li, 2000). We can only speculate on the origin of this, somewhat minor, discrepancy between these results and ours. One possible explanation is that we applied muscimol directly to the region that contains the Phox2b$^+$TH$^-$ cells using fine-tipped pipettes and electrophysiological coordinates whereas Nattie & Li used a dialysis probe which may have delivered the drug to a slightly different set of neuronal targets because of its large size. Another obvious difference is that our rats were anaesthetized. Finally, muscimol produced a tendency towards hypothermia and reduced oxygen consumption in the Nattie & Li study (Nattie & Li, 2000) which could have accounted for the slight reduction in V_T that was observed (Mortola & Frappell, 2000).

More serious discrepancies come to mind when one considers that unilateral lesions of the RTN using DC current or an excitoxin (kainic acid, ibotenic acid) produce large decreases in phrenic nerve activity and its response to CO_2 in anaesthetized cats and rats (Nattie *et al.* 1991; Nattie & Li, 1994). Several reasons can be proposed. With regard to the effects of electrical lesions, consideration should be given to the fibres of passage. The RTN region is a major highway for axons linking the ventral respiratory group and the NTS on one hand and the parabrachial region on the other (e.g. Ezure *et al.* 2003; Alheid *et al.* 2004; Takakura *et al.* 2006, 2007). Interruption of these connections could have contributed to the effect produced by lesioning the RTN region. As for the excitotoxins, which are powerful glutamate receptor agonists, they produce depolarizing blockade at the site of injection and persistent neuronal stimulation further away. The effect of such drugs is very difficult to interpret since a steady-state condition is never obtained during the course of an acute experiment and the extent of the damage cannot be assessed histologically before 1 or 2 days. We speculate that unilateral injection of excitotoxin into the RTN region inhibits the phrenic nerve discharge by several mechanisms including depolarization blockade of some of the RTN neurons and activation of adjacent structures such as the Bötzinger or A5 regions which contain neurons that inhibit breathing (Monnier *et al.* 2003; Rybak *et al.* 2004; Hilaire *et al.* 2004).

The destruction of the Phox2b$^+$TH$^-$ neurons may account for the respiratory deficits caused by injection of SSP-SAP into the RTN

SSP-SAP is a ribosome-inactivating toxin that has been designed to enter cells primarily by internalization of the

agonist-liganded substance P receptor (Wiley & Kline, 2000). Although, in the RTN, very little NK1R immuno-reactivity is visibly associated with the cell bodies of the $Phox2b^+TH^-$ neurons, some form of neurokinin receptor is clearly present on the surface of these neurons because they are strongly activated by substance P both *in vivo* and *in vitro* (Mulkey *et al.* 2007*a*). The destruction of RTN $Phox2b^+TH^-$ neurons by SSP-SAP is presumably due to the presence of these receptors.

The fact that the $Phox2b^+TH^-$ cells are destroyed by SSP-SAP is necessary evidence that the loss of these neurons could be responsible for the respiratory deficits identified in this and previous studies in which the toxin was injected in the RTN (Nattie & Li, 2002). This interpretation is reinforced by the existence of a correlation between the increase in apnoeic threshold and the percentage loss of the $Phox2b^+TH^-$ cells. We cannot exclude the possibility that the respiratory deficits caused by injecting SSP-SAP into the RTN could have also resulted from the destruction of cells other than the $Phox2b^+TH^-$ neurons but several reasons reduce the plausibility of this interpretation. First, while not specific, the toxin exhibited distinct selectivity. For example, the nearby catecholaminergic and serotonergic neurons were unaffected and the facial and ambigual motor neurons that reside just dorsal to the RTN were also essentially intact. Importantly, our densitometry analysis indicated that NK1R-expressing neurons located within the ventral respiratory column at the level of the pre-Bötzinger complex and caudal to this level were intact. Selectivity does not mean specificity, however. We found evidence of neuronal damage at the rostral end of the Bötzinger region and in the parapyramidal region medial to the RTN where a group of highly NK1R-ir neurons was consistently destroyed (Fig. 3). However, we also obtained evidence that the collateral damage present in these regions is unlikely to account for the respiratory deficits that we observed.

Damage to the Bötzinger region is unlikely to explain the rise in the apnoeic threshold because the magnitude of this rise was greatly increased by injecting SSP-SAP into additional sites located at least $600 \mu m$ rostral to the Bötzinger region. These additional lesions raised the kill rate of the $Phox2b^+TH^-$ neurons by another 13% on average without increasing the damage caused by the toxin at the level of the Bötzinger region. Because the rostral cluster of $Phox2b^+TH^-$ neurons was still intact in the animals subjected to such quadruple lesions, it can be safely assumed that the toxin does little or no damage at a distance of more than a few hundred micrometres from the centre of the injection.

Damage to the parapyramidal region is also unlikely to have accounted for the respiratory effects of SSP-SAP as suggested by the muscimol experiments. Indeed, in rats with lesions of the left RTN, contralateral muscimol injection into the parapyramidal region produced no effect on respiration (Fig. 4) whereas muscimol injections placed accurately among the $Phox2b^+TH^-$ neurons caused instant phrenic apnoea (Fig. 4). Thus, there is no evidence that the parapyramidal region plays a significant role in the central chemoreflex, at least under our experimental conditions.

Unilateral injection of muscimol into the RTN on the side contralateral to an SSP-SAP lesion produced a far greater reduction of the chemoreflex than chronic bilateral lesions of up to 70% of the $Phox2b^+TH^-$ neurons. A muscimol injection placed into the centre of the caudal cluster of $Phox2b^+TH^-$ neurons is likely to have inhibited a large majority of these cells on the intact side while the SSP-SAP lesion had destroyed about 65% of the cells on the contralateral side in these rats. Therefore, on average, the percentage of impaired $Phox2b^+TH^-$ neurons should have been approximately equal with both protocols. The fact that chronic lesions produce less intense deficits than the acute inhibition of about the same proportion of the cells could have several explanations. The most likely is that, after chronic lesions, the surviving $Phox2b^+TH^-$ cells develop new connections that make them more effective. Another explanation, also implying some form of plasticity, is that central chemoreceptors located elsewhere compensate for the loss of the RTN neurons.

In brief, SSP-SAP destroyed the RTN $Phox2b^+TH^-$ neurons with considerable though incomplete selectivity. The collateral damage present in the Bötzinger region and in the rostral parapyramidal region is unlikely to account for the respiratory deficits caused by injection of SSP-SAP directly into the RTN. The results suggest that the chemo-reflex attenuation produced by chronic bilateral injections of SSP-SAP into the RTN is likely to be due to the loss of the $Phox2b^+TH^-$ neurons in this area. The central apnoea caused by unilateral injection of muscimol into RTN on the side contralateral to an SSP-SAP lesion is also probably related to the inhibition of a large fraction of the $Phox2b^+TH^-$ neurons.

Interpreting the breathing deficits caused by SSP-SAP

Unlike plethysmographic measurements, the neural equivalent of the minute $\times$ volume (we referred to this as mvPND) is not readily comparable across groups of rats because PND is a multiunit activity that is not measured in absolute terms. Therefore, in all rats in which CO_2 induces some PND, the relationship between PND and end-expiratory CO_2 converges at the same level of one arbitrary unit at high levels of CO_2 (Fig. 5*C*), even if the 'real' maximum PND was considerably lower at saturation in the lesioned rats. This inevitable normalization also impacts on the slope of the relationship between PND and end-expiratory CO_2, which therefore cannot be directly compared between groups either. The only dependent

variable that could be measured in an unbiased way in the present experiment was the apnoeic threshold. This value was increased by a robust amount in the rats with the most extensive lesions of the $Phox2b^+TH^-$ cells. Does this change mean that the central chemoreflex was attenuated? If one defines the central chemoreflex as the percentage increase in PND caused by a given increment of CO_2 without consideration for the apnoeic threshold, one could conclude that the SSP-SAP lesions that we made did not change the sensitivity of this reflex. If one defines the chemoreflex as the increase in PND caused by a given increment of CO_2 above the apnoeic threshold of the control rats, one would conclude that the lesions had a very large depressant effect on the chemoreflex.

The study most directly comparable to ours is that of Nattie & Li (2002) in which rats were examined while awake 2 weeks after bilateral injection of a very similar toxin into the RTN region (substance P–saporin). These animals had a decreased ventilation at rest, an increased arterial P_{CO_2} at rest and a lesser degree of ventilatory stimulation when they were exposed to CO_2 and these effects were not state dependent. These results are consistent with the partial destruction of a group of neurons that contributes at all times a pH-sensitive drive to breathe and this interpretation is in perfect register with the physiological properties of the $Phox2b^+TH^-$ cells (e.g. Rosin *et al.* 2006; Takakura *et al.* 2006; Guyenet *et al.* 2008). If RTN neurons contribute a significant portion of the pH-dependent drive to breathe, a partial lesion of these cells would be expected to raise the apnoeic threshold under anaesthesia because, under such conditions, breathing is predominantly driven by CO_2 as opposed to feed-forward influences from suprapontine structures and the integrity of RTN is required for CO_2 to be able to drive breathing (Takakura *et al.* 2006). Two weeks after the RTN lesions Nattie & Li (2002) found a relatively modest reduction in the ventilatory increase ($\Delta \dot{V}_E$) caused by CO_2. In fact this increase was, percentage-wise, at most equivalent to the percentage reduction of the resting ventilation, $\dot{V}_E$, which raises the same issue as to whether these lesions lower the drive to breathe or the chemoreflex. As indicated above, our data cannot strictly evaluate the change in chemoreflex slope and the increased slope of the relationship between PND and end-expiratory CO_2 that we show in Fig. 5 does not necessarily indicate that the chemoreflex of the lesioned rats was facilitated. Thus, we see no discrepancy between our results obtained under anaesthesia and those of Nattie & Li (2002) in awake rats and we propose that, given what is known of the cellular properties of the $Phox2b^+TH^-$ neurons, the results of both studies can be explained very satisfactorily by the theory that RTN neurons contribute a pH-modulated excitatory drive to the central pattern generator and that, in both studies this cell population was only partially lesioned.

How important are the $Phox2b^+TH^-$ neurons of RTN for breathing automaticity and CO_2 homeostasis in the adult?

The selective loss of a large portion of the RTN $Phox2b^+$ neurons in the mouse is the possible cause of a total absence of respiratory response to CO_2 at birth, which results in asphyxia and death (Dubreuil *et al.* 2008). One interpretation of these results is that, at least during the neonatal period, the pH-regulated excitatory drive that the central pattern generator receives from the $Phox2b^+$ neurons of RTN defines both breathing intensity and its stimulation by arterial P_{CO_2}.

The present experiments are insufficient to prove the validity of this theory in the case of the adult but they suggest that the hypothesis is viable and should be explored further. Indeed, a large increase in apnoeic threshold was produced in our rat model by destroying a comparable percentage of RTN $Phox2b^+TH^-$ neurons than in the genetic model of Dubreuil *et al.* (2008). Dubreuil and colleagues, however, measured the number of neurons that coexpress Phox2b and VGLUT2. This population includes the C1 neurons (Stornetta *et al.* 2002, 2006), the number of which is unaffected by the Phox2b mutation (Dubreuil *et al.* 2008). The presence of many C1 neurons in the RTN may have lead these authors to underestimate the percentage loss of the putative chemorecetors i.e. the $Phox2b^+TH^-$ neurons. In our model, the relationship between the apnoeic threshold and the kill rate of the $Phox2b^+TH^-$ neurons was clearly non-linear. The loss of up to 57% of these cells had a very modest effect on the apnoeic threshold whereas a large elevation of this threshold resulted from increasing the kill rate to around 70%. The fact that a high kill rate would be required to produce symptoms is expected. Parkinson's disease becomes symptomatic only with the loss of about 80% of the dopaminergic neurons (Schulz & Falkenburger, 2004) and the destruction of well over 80% of the C1 neurons is required to produce chronic hypotension and a cohort of associated autonomic deficits (Madden *et al.* 2006). The loss of the RTN $Phox2b^+TH^-$ neurons that was produced in the present study (70%) was therefore still comparatively light by these standards. This fact plausibly accounts for the survivability of these lesions and suggests that a higher kill rate of the RTN $Phox2b^+TH^-$ neurons may have respiratory consequences in the adult that are as serious as in the genetic model of Dubreuil *et al.* (2008), namely severe apnoea and perhaps death. However, the performance of such experiments in the adult raises ethical concerns and, for this reason, they were not attempted. A different methodology will have to be implemented to determine how critical the RTN is to breathing in adult rodents.

Summary and conclusions

The RTN of the adult rat contains around 2100 $Phox2b^+TH^-$ neurons spread out over 2 mm in the rostrocaudal direction. These neurons are destroyed with considerable though imperfect selectivity by injecting the toxin SSP-SAP in their midst. The breathing deficit produced by destroying the RTN region with SSP-SAP correlates with the percentage destruction of the $Phox2b^+TH^-$ neurons and could therefore be due to the loss of these particular neurons. The results of these present experiments are consistent with the notion that the RTN contributes an important pH-regulated excitatory drive to the respiratory pattern generator (Nattie & Li, 2002) and that the $Phox2b^+TH^-$ neurons are responsible for this aspect of the function of this nucleus.

References

Abercrombie M (1946). Estimation of nuclear population from microtome sections. *Anat Rec* **94**, 239–247.

Alheid GF, Milsom WK & McCrimmon DR (2004). Pontine influences on breathing: an overview. *Respir Physiol Neurobiol* **143**, 105–114.

Amiel J, Laudier B, Attie-Bitach T, de Trang HPL, Gener B, Trochet D, Etchevers H, Ray P, Simonneau M, Vekemans M, Munnich A, Gaultier C & Lyonnet S (2003). Polyalanine expansion and frameshift mutations of the paired-like homeobox gene *PHOX2B* in congenital central hypoventilation syndrome. *Nat Genet* **33**, 459–461.

Dubreuil V, Ramanantsoa N, Trochet D, Vaubourg V, Amiel J, Gallego J, Brunet JF & Goridis C (2008). A human mutation in Phox2b causes lack of CO_2 chemosensitivity, fatal central apnea and specific loss of parafacial neurons. *Proc Natl Acad Sci U S A* **105**, 1067–1072.

Ezure K, Tanaka I & Saito Y (2003). Brainstem and spinal projections of augmenting expiratory neurons in the rat. *Neurosci Res* **45**, 41–51.

Feldman JL & Del Negro CA (2006). Looking for inspiration: new perspectives on respiratory rhythm. *Nat Rev Neurosci* **7**, 232–242.

Feldman JL, Mitchell GS & Nattie EE (2003). Breathing: rhythmicity, plasticity, chemosensitivity. *Annu Rev Neurosci* **26**, 239–266.

Gray PA, Janczewski WA, Mellen N, McCrimmon DR & Feldman JL (2001). Normal breathing requires preBotzinger complex neurokinin-1 receptor-expressing neurons. *Nat Neurosci* **4**, 927–930.

Guyenet PG, Bayliss DA, Mulkey DK, Stornetta RL, Moreira TS & Takakura AT (2008). The retrotrapezoid nucleus and central chemoreception. *Adv Exp Med Biol* **605**, 327–332.

Guyenet PG, Mulkey DK, Stornetta RL & Bayliss DA (2005). Regulation of ventral surface chemoreceptors by the central respiratory pattern generator. *J Neurosci* **25**, 8938–8947.

Hilaire G, Viemari JC, Coulon P, Simonneau M & Bevengut M (2004). Modulation of the respiratory rhythm generator by the pontine noradrenergic A5 and A6 groups in rodents. *Respir Physiol Neurobiol* **143**, 187–197.

Janczewski WA & Feldman JL (2006). Distinct rhythm generators for inspiration and expiration in the juvenile rat. *J Physiol* **570**, 407–420.

Kang BJ, Chang DA, Mackay DD, West GH, Moreira TS, Takakura AC, Gwilt JM, Guyenet PG & Stornetta RL (2007). Central nervous system distribution of the transcription factor Phox2b in the adult rat. *J Comp Neurol* **503**, 627–641.

Madden CJ, Stocker SD & Sved AF (2006). Attenuation of homeostatic responses to hypotension and glucoprivation after destruction of catecholaminergic rostral ventrolateral medulla (RVLM) neurons. *Am J Physiol Regul Integr Comp Physiol* **291**, R751–R759.

Monnier A, Alheid GF & McCrimmon DR (2003). Defining ventral medullary respiratory compartments with a glutamate receptor agonist in the rat. *J Physiol* **548**, 859–874.

Moreira TS, Takakura AC, Colombari E & Guyenet PG (2006). Central chemoreceptors and sympathetic vasomotor outflow. *J Physiol* **577**, 369–386.

Moreira TS, Takakura AC, Colombari E, West GH & Guyenet PG (2007). Inhibitory input from slowly adapting lung stretch receptors to retrotrapezoid nucleus chemoreceptors. *J Physiol* **580**, 285–300.

Mortola JP & Frappell PB (2000). Ventilatory responses to changes in temperature in mammals and other vertebrates. *Annu Rev Physiol* **62**, 847–874.

Mulkey DK, Rosin DL, West G, Takakura AC, Moreira TS, Bayliss DA & Guyenet PG (2007*a*). Serotonergic neurons activate chemosensitive retrotrapezoid nucleus neurons by a pH-independent mechanism. *J Neurosci* **27**, 14128–14138.

Mulkey DK, Stornetta RL, Weston MC, Simmons JR, Parker A, Bayliss DA & Guyenet PG (2004). Respiratory control by ventral surface chemoreceptor neurons in rats. *Nat Neurosci* **7**, 1360–1369.

Mulkey DK, Talley EM, Stornetta RL, Siegel AR, West GH, Chen X, Sen N, Mistry AM, Guyenet PG & Bayliss DA (2007*b*). TASK channels determine pH sensitivity in select respiratory neurons but do not contribute to central respiratory chemosensitivity. *J Neurosci* **27**, 14049–14058.

Nattie EE & Li A (1994). Retrotrapezoid nucleus lesions decrease phrenic activity and CO_2 sensitivity in rats. *Respir Physiol* **97**, 63–77.

Nattie E & Li A (2000). Muscimol dialysis in the retrotrapezoid nucleus region inhibits breathing in the awake rat. *J Appl Physiol* **89**, 153–162.

Nattie EE & Li A (2002). Substance P-saporin lesion of neurons with NK1 receptors in one chemoreceptor site in rats decreases ventilation and chemosensitivity. *J Physiol* **544**, 603–616.

Nattie E & Li A (2006). Central chemoreception 2005: a brief review. *Auton Neurosci* **126–127**, 332–338.

Nattie G & Li A (2008). Multiple central chemoreceptor sites: cell types and function in vivo. *Adv Exp Med Biol* **605**, 343–347.

Nattie EE, Li A, Richerson G & Lappi DA (2004). Medullary serotonergic neurones and adjacent neurones that express neurokinin-1 receptors are both involved in chemoreception *in vivo*. *J Physiol* **556**, 235–253.

Nattie EE, Li AH & St John WM (1991). Lesions in retrotrapezoid nucleus decrease ventilatory output in anesthetized or decerebrate cats. *J Appl Physiol* **71**, 1364–1375.

Onimaru H & Homma I (2003). A novel functional neuron group for respiratory rhythm generation in the ventral medulla. *J Neurosci* **23**, 1478–1486.

Onimaru H, Kumagawa Y & Homma I (2006). Respiration-related rhythmic activity in the rostral medulla of newborn rats. *J Neurophysiol* **96**, 55–61.

Paxinos G & Watson C (1998). *The Rat Brain in Stereotaxic Coordinates*, 4th edn. Academic press, San Diego.

Rosin DL, Chang DA & Guyenet PG (2006). Afferent and efferent connections of the rat retrotrapezoid nucleus. *J Comp Neurol* **499**, 64–89.

Rybak IA, Shevtsova NA, Paton JF, Dick TE, St-John WM, Morschel M & Dutschmann M (2004). Modeling the ponto-medullary respiratory network. *Respir Physiol Neurobiol* **143**, 307–319.

Schulz JB & Falkenburger BH (2004). Neuronal pathology in Parkinson's disease. *Cell Tissue Res* **318**, 135–147.

Stornetta RL & Guyenet PG (1999). Distribution of glutamic acid decarboxylase mRNA-containing neurons in rat medulla projecting to thoracic spinal cord in relation to monoaminergic brainstem neurons. *J Comp Neurol* **407**, 367–380.

Stornetta RL, Moreira TS, Takakura AC, Kang BJ, Chang DA, West GH, Brunet JF, Mulkey DK, Bayliss DA & Guyenet PG (2006). Expression of Phox2b by brainstem neurons involved in chemosensory integration in the adult rat. *J Neurosci* **26**, 10305–10314.

Stornetta RL, Sevigny CP, Schreihofer AM, Rosin DL & Guyenet PG (2002). Vesicular glutamate transporter DNPI/GLUT2 is expressed by both C1 adrenergic and nonaminergic presympathetic vasomotor neurons of the rat medulla. *J Comp Neurol* **444**, 207–220.

Taccola G, Secchia L & Ballanyi K (2007). Anoxic persistence of lumbar respiratory bursts and block of lumbar locomotion in newborn rat brainstem–spinal cords. *J Physiol* 585, 507–524.

Takakura AC, Moreira TS, Colombari E, West GH, Stornetta RL & Guyenet PG (2006). Peripheral chemoreceptor inputs to retrotrapezoid nucleus (RTN) CO_2-sensitive neurons in rats. *J Physiol* **572**, 503–523.

Takakura AC, Moreira TS, West GH, Gwilt JM, Colombari E, Stornetta RL & Guyenet PG (2007). GABAergic pump cells of solitary tract nucleus innervate retrotrapezoid nucleus chemoreceptors. *J Neurophysiol* **98**, 374–381.

Wang H, Germanson TP & Guyenet PG (2002). Depressor and tachypneic responses to chemical stimulation of the ventral respiratory group are reduced by ablation of neurokinin-1 receptor-expressing neurons. *J Neurosci* **22**, 3755–3764.

Weese-Mayer DE, Berry-Kravis EM & Marazita ML (2005). In pursuit (and discovery) of a genetic basis for congenital central hypoventilation syndrome. *Respir Physiol Neurobiol* **149**, 73–82.

Wiley RG & Kline RH IV (2000). Neuronal lesioning with axonally transported toxins. *J Neurosci Methods* **103**, 73–82.

Williams RW & Rakic P (1988). Three-dimensional counting: an accurate and direct method to estimate numbers of cells in sectioned material. *J Comp Neurol* **278**, 344–352.

Acknowledgements

Supplemental material

Online supplemental material for this paper can be accessed at: http://jp.physoc.org/cgi/content/full/jphysiol.2008.153163/DC1 and

http://www.blackwell-synergy.com/doi/suppl/10.1113/jphysiol.2008.153163